

# PCCP

Accepted Manuscript



This is an *Accepted Manuscript*, which has been through the Royal Society of Chemistry peer review process and has been accepted for publication.

*Accepted Manuscripts* are published online shortly after acceptance, before technical editing, formatting and proof reading. Using this free service, authors can make their results available to the community, in citable form, before we publish the edited article. We will replace this *Accepted Manuscript* with the edited and formatted *Advance Article* as soon as it is available.

You can find more information about *Accepted Manuscripts* in the [Information for Authors](#).

Please note that technical editing may introduce minor changes to the text and/or graphics, which may alter content. The journal's standard [Terms & Conditions](#) and the [Ethical guidelines](#) still apply. In no event shall the Royal Society of Chemistry be held responsible for any errors or omissions in this *Accepted Manuscript* or any consequences arising from the use of any information it contains.

**Unraveling the Complex Chemistry Using Dimethylsilane as a Precursor Gas in Hot Wire  
Chemical Vapor Deposition**

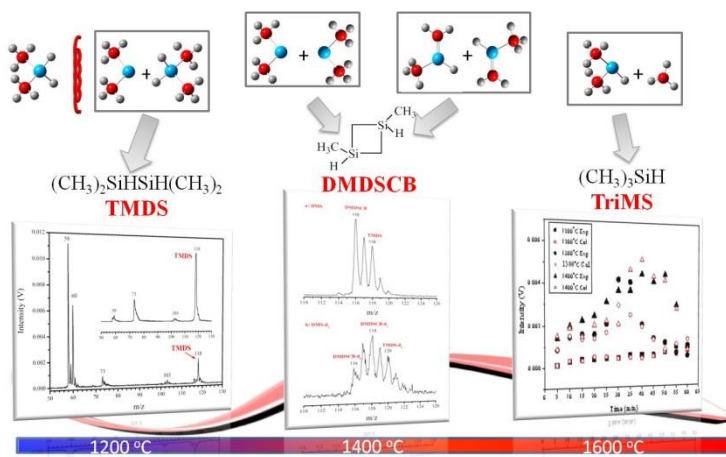
Rim Toukabri, Yujun Shi\*

Department of Chemistry, University of Calgary, Calgary, Alberta, T2N 1N4 Canada

\* Corresponding Author: Yujun Shi, Tel: 1-403-2108674; Fax: 1-403-2899488; Email:  
shiy@ucalgary.ca.

## Table of contents entry

At low filament temperatures and short reaction time, silylene chemistry dominates. The free-radical reactions become more important with increasing temperature and time.



**Abstract**

The gas-phase reaction chemistry when using dimethylsilane as a source gas in a hot-wire chemical vapor deposition (CVD) process has been studied in this work. The complex chemistry is unraveled by using a soft 10.5 eV single photon ionization techniques coupled with time-of-flight mass spectrometry in combination with the isotope labelling and chemical trapping methods. It has been demonstrated that both free-radical reactions and those involving silylene/silene intermediates are important. The reaction chemistry is characterized by the formation of 1,1,2,2-tetramethyldisilane (TMDS) from dimethylsilylene insertion into the Si-H bond of DMS, trimethylsilane (TriMS) from free-radical recombination, and 1,3-dimethyl-1,3-disilacyclobutane (DMDSCB) from the self dimerization of either dimethylsilylene and 1-methylsilylene. At low filament temperatures and short reaction time, silylene chemistry dominates. The free-radical reactions become more important with increasing temperature and time. The same three products have been detected when using tantalum and tungsten filaments, indicating that changing filament material from Ta to W does not affect much the gas-phase reaction chemistry when using DMS as a source gas in a hot-wire CVD reactor.

## Introduction

Several studies have been reported on the pyrolysis of dimethylsilane (DMS) under different conditions, such as static flow,<sup>1</sup> stirred flow and shock tube,<sup>2,3</sup> and high-pressure thermal decomposition.<sup>4</sup> Although the products varied, one discovery in common is that both a free-radical process and a molecular elimination mechanism are operative in the pyrolysis of DMS. The primary free radicals were formed from the cleavage of Si-H or Si-CH<sub>3</sub> bond, which served to initiate a short-chain reaction. The unimolecular elimination of H<sub>2</sub> and methane molecules were the predominant dissociation reactions that led to the formation of silylenes (:SiH(CH<sub>3</sub>) and :Si(CH<sub>3</sub>)<sub>2</sub>) as the major products along with silene isomers. Rickborn *et al.*<sup>3</sup> have shown that methane elimination accounts for about 17% and 19% of the total primary dissociation under stirred flow and shock tube conditions, respectively. In a study on the 147-nm photolysis of DMS, the molecular elimination to produce silylene species was also found to be the major pathway of decomposition.<sup>5</sup>

Despite its simple structure, DMS has received less attention than other methyl-substituted silane molecules as a possible precursor in the chemical vapor deposition (CVD) of silicon carbide (Si<sub>1-x</sub>C<sub>x</sub>) thin films.<sup>6-10</sup> In an attempt to study the growth mechanism of Si<sub>1-x</sub>C<sub>x</sub> using DMS as a source gas in Catalytic-CVD (Cat-CVD, also known as hot-wire CVD), Nakayama *et al.*<sup>9</sup> examined the composition of Si-C alloy produced using different filament materials (W, Ta, Mo, Pt) at different temperatures. They found that the C content (C/(Si+C)) in Si-C alloy films was the highest for Pt. They postulated that DMS decomposed on Ta and W to produce small hydrogenated silicon carbon species, whereas Mo and Pt dissociated DMS less effectively to large hydrogenated silicon carbon species. Zaharias *et al.*<sup>10</sup> identified the gas-phase decomposition products of several single-source precursors, including mono-, di-, tri-, and tetra-

methylsilanes, from the heated W or Re filament. The major products released from the filaments with all precursors were found to be Si and CH<sub>3</sub> radicals. In correlating the hot-wire decomposition chemistry with the concomitant Si<sub>1-x</sub>C<sub>x</sub> film growth, they found that SiH<sub>2</sub> groups were dominant in the films grown from mono-, di-, and tri-methylsilane.<sup>11</sup> The silicon hydride was originated from the hydrogenation of Si radicals, which were formed in the gas phase. The role of methyl radicals in the Si<sub>1-x</sub>C<sub>x</sub> film formation processes is not clear. It should be noted that the deposition in the latter work is under a much lower pressure ( $5 \times 10^{-6}$  Torr) than those (7.5-75 mTorr) used in Nakayama's work.

To understand the reaction chemistry of DMS in the presence of a hot metal filament under different pressures, the primary decomposition and secondary gas-phase reaction products along with their formation mechanisms with both W and Ta filaments have been studied in this work. This constitutes part of our ongoing efforts on the gas-phase reaction chemistry assumed by various single-source organosilicon precursors in the process of hot-wire CVD. Our previous studies on trimethylsilane<sup>12,13</sup> and tetramethylsilane<sup>14</sup> have shown that free-radical chain reactions dominate in the secondary gas-phase reactions with these two precursors when using W filaments. The reactive silene intermediates are also involved, but their contributions were minor. This current work will answer the important question of how reaction chemistry changes with the increasing number of Si-H bonds in DMS. Most of the studies using methyl-substituted silane precursors to form Si<sub>1-x</sub>C<sub>x</sub> films with hot-wire CVD opt for a W filament due to its high melting point and low price. However, W filaments suffer from a short lifetime, especially at lower filament temperatures.<sup>15-18</sup> In contrast, a Ta filament lasts longer since it is less prone to form silicides on its surface.<sup>19,20</sup> Despite this advantage, little is known about the gas-phase chemistry when using these precursor molecules with Ta as a filament. Therefore, we have studied the gas-

phase chemistry of DMS on a Ta filament, and the results are compared with that on a W filament.

In this work, detection of DMS decomposition products under a low pressure of  $1.0 \times 10^{-5}$  Torr provides information on the species released directly from the hot filament made of either W or Ta since the low pressure gives a collision-free condition. Mixtures with concentrations of 1% and 4% DMS seeded in He were used for the detection of gas-phase secondary reaction products with a total gas pressure of 12 Torr in a hot-wire CVD reactor. The diagnostic tool used in this work to probe the chemical species is nonresonant 10.5 eV vacuum ultraviolet (VUV) single photon ionization (SPI) in tandem with a time-of-flight mass spectrometry (TOF MS).<sup>21,22</sup> This is combined with isotope labeling and chemical trapping to unravel the complex chemistry in the reactor setup. Specifically, experiments with the deuterated isotopomer,  $(\text{CH}_3)_2\text{SiD}_2$  (DMS- $\text{d}_2$ ), were performed to assist in the identification of reaction products formed. 1,3-butadiene was used to trap silylene and silene species, which serves to differentiate the mechanism involving silylene/silene intermediates from the free-radical processes. A comparison of the reaction chemistry using DMS with those of trimethylsilane and tetramethylsilane is made to shed lights on the effect of increasing number of Si-H bonds in the precursor molecules. The effect of filament material on the gas-phase reaction chemistry is also discussed.

## Experimental methods

The experimental setup of the hot-wire CVD sources and the 10.5 eV VUV laser SPI TOF mass spectrometer used to study the gas-phase reaction chemistry in the hot-wire CVD processes have been described elsewhere.<sup>23,24</sup> Briefly, a collision-free hot-wire CVD source was

employed for the detection of primary decomposition products of DMS from the heated W or Ta filament. Here, a resistively heated filament (10 cm length, 0.5 mm diameter) was placed in the main ionization chamber housing the linear TOF mass spectrometer. The operating pressure in the main chamber was maintained at  $\sim 1.0 \times 10^{-5}$  Torr to ensure collision-free conditions.

Filament temperatures in the range of 900 to 2200 °C were investigated at increments of 100 °C. To examine the products from secondary gas-phase reactions, a cylindrical hot-wire CVD reactor with a resistively heated filament was used. The filament temperature was measured by a two-color pyrometer (Chino Works). The total pressure of a mixture of DMS and helium in the reactor monitored by a capacitance manometer (MKS, Baratron, type 626A) was maintained at 12 Torr using a mass flow controller (MKS, type 1179A). The partial pressure of DMS (or DMS- $d_2$ ) sample in the reactor was 0.12 Torr and 0.48 Torr, respectively, when using a 1% and 4% sample mixtures in He. The reactor was connected to the main chamber through a 0.15 mm diameter pinhole. Gas-phase reaction products were examined at filament temperatures varying from 900 to 1800 °C at increments of 100 °C. For each temperature, a mass spectrum was recorded every 5 min for 1 h.

The chemical products from primary decomposition on the hot filament using the collision-free CVD source or from secondary gas-phase reactions in the CVD reactor were ionized by the 118 nm VUV laser radiation (10.5 eV). The ionization laser radiation was generated in a non-resonant third harmonic process of the 355-nm UV output from an Nd:YAG laser (Spectra-Physics, LAB-170-10) in a gas cell filled with 210 Torr of 10:1 Ar:Xe gas mixture. A lithium fluoride lens was positioned in the optical path to focus the 118-nm VUV radiation at the center of the ionization region in the TOF mass spectrometer. The residual 355-nm UV beam was caused to diverge in the same region due to the dependence of focal length on



wavelength. Signals from a two-stage microchannel plate (MCP) detector were preamplified, averaged over 512 laser pulses, and displayed on a digital oscilloscope before being saved in a computer for analysis.

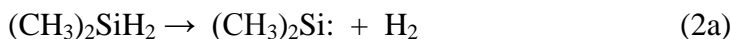
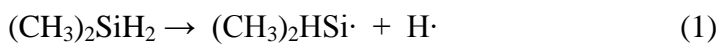
W (99.9+%, Aldrich) and Ta (99.9+%, Aldrich) were used as filament materials. DMS (ABCR, 97%) was used without further purification. Its deuterated isotopomer,  $(\text{CH}_3)_2\text{SiD}_2$  (DMS- $\text{d}_2$ ), was synthesized by the reduction of dimethyldichlorosilane  $((\text{CH}_3)_2\text{SiCl}_2)$  with an excess of lithium aluminum deuteride ( $\text{LiAlD}_4$ , CDN Isotopes, 98 atom% D).<sup>25</sup> Due to the high volatility of DMS- $\text{d}_2$ , its isotope purity (95%) was examined mainly with our TOF mass spectrometer. Gaseous mixtures of DMS (or DMS- $\text{d}_2$ ) in He (99.999%, Praxair) having different concentrations of 1% and 4% were prepared by diluting the room-temperature DMS (or DMS- $\text{d}_2$ ) sample in He in a 2.25-liter sample cylinder.

## Results and discussion

### 1. Primary decomposition on Ta and W filaments

In determining the primary decomposition products of DMS on a Ta or W filament, it was found that two new mass peaks at  $m/z$  2 and 15, representing  $\text{H}_2^+$  and  $\text{CH}_3^+$ , appeared after the filament was turned on. Their intensities increased with filament temperatures. The mechanism for the formation of  $\text{H}_2$  molecule and methyl radical from DMS along with other three methyl-substituted silane molecules has been discussed in detail in our previous work.<sup>26</sup> It has been shown that DMS dissociatively adsorbed on Ta and W filaments by Si-H bond cleavage. This is followed by Si- $\text{CH}_3$  bond breaking to form methyl radical or by recombination of H adsorbates to form  $\text{H}_2$  molecule. The formation of  $\cdot\text{H}$  radical was also demonstrated when methyl-substituted silanes, including DMS, were used as precursor gases.

In order to understand the concomitant products with the formation of  $\cdot\text{H}$  and  $\text{H}_2$ , the intensity ratios of possible complimentary fragment peaks to that of the parent ion peak ( $m/z$  60) were examined. Figure 1 shows the intensity ratios of  $(\text{CH}_3)_2\text{HSi}^+$  ( $m/z$  59) and  $\text{C}_2\text{H}_6\text{Si}^+$  ( $m/z$  58), respectively, to that of the parent DMS ion at different W filament temperatures at a chamber pressure of  $1.0 \times 10^{-5}$  Torr. Both ratios increased with W filament temperature (same for Ta), indicating the presence of dimethylsilyl radical ( $(\text{CH}_3)_2\text{HSi}\cdot$ , Eqn. 1) and a species with an elemental composition of  $\text{C}_2\text{H}_6\text{Si}$  in the gas phase. The latter species, being the co-product of  $\text{H}_2$ , can be dimethylsilylene or methylsilylene (both having a mass of 58 amu), depending on whether the second H is cleaved from Si-H or C-H bonds (Eqn. 2).



## 2. Gas-phase reactions in a hot-wire CVD reactor with a Ta filament

The gas-phase reaction chemistry when using DMS as a precursor gas in a hot-wire CVD reactor was studied by monitoring the exiting chemical products that were generated from the secondary gas-phase reactions between the primary decomposition species on the filament and the parent DMS molecules. Figure 2 shows the TOF mass spectra recorded after the filament was turned on for 10 min for 12 Torr of 1% DMS/He sample at different filament temperatures between 1200 and 1600 °C. After the Ta filament was turned on, the parent and its photofragment ion peak [ $\text{Si}(\text{CH}_3)_2^+$  ( $m/z$  58)], dominated in the room-temperature mass spectrum of DMS decreased with increasing filament temperature, indicating that the parent DMS molecules were decomposed on the filament and consumed in secondary gas-phase reactions in

the reactor. This decrease was observed to start at 1100 °C when using 12 Torr of 1% DMS/He mixture ( $P_{\text{DMS}} = 0.12$  Torr). With an increase in the DMS partial pressure to 0.48 Torr (12 Torr of 4% DMS/He sample), this temperature is decreased to 1000 °C. The temperature at which the chemistry of DMS starts in a reactor setup is lower than those for TriMS,<sup>12</sup> TMS,<sup>14</sup> and HMDS,<sup>23</sup> but slightly higher than or comparable to those when using four-membered-ring compounds, *i.e.*, silacyclobutane,<sup>27</sup> 1-methyl-1-silacyclobutane,<sup>24</sup> and 1,1-dimethyl-1-silacyclobutane.<sup>28</sup>

As shown in Figure 2, a variety of new mass peaks appeared after the filament was turned on, *e.g.*, those at  $m/z$  73, 88, 103, 116, and 118, when the intensity of the parent molecule decreased. Figure 3 shows the intensity distribution of the three main peaks at  $m/z$  73, 116 and 118 when using 0.12 Torr of DMS at different filament temperatures. Both filament-on time and filament temperature play a role in determining the relative intensities of these peaks. At a relatively low temperature of 1200 °C, the peak at  $m/z$  118 is dominating at  $t \leq 30$  min, beyond this time, there is an increase in the peak intensity at  $m/z$  73. As the filament temperature is increased to 1300 and 1400 °C, the time when the peak at  $m/z$  118 is dominant is shortened to 25 min and 10 min, respectively. The peaks at  $m/z$  73 and 116 become more important beyond. At a higher temperature of 1600 °C, the peak at  $m/z$  73 predominates all the time. Same is true for the higher-pressure DMS sample of 0.48 Torr. A detailed discussion on the formation of these main products is presented in the following sections.

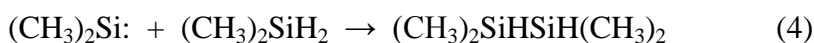
In the discussions below, the abbreviations of the compound names are used for brevity. Table 1 lists the compound abbreviations along with their corresponding names and structures.

Table 1. The structures, names, and abbreviations of compounds used in this work

Compound structure	Compound Name	Abbreviations
$(\text{CH}_3)_2\text{SiH}_2$	dimethylsilane	DMS
$(\text{CH}_3)_2\text{SiHSiH}(\text{CH}_3)_2$	1,1,2,2-tetramethyldisilane	TMDS
$\text{CH}_2=\text{CHCH}=\text{CH}_2$	1,3-butadiene	BTD
$(\text{CH}_3)_3\text{SiH}$	trimethylsilane	TriMS
$(\text{CH}_3)_4\text{Si}$	tetramethylsilane	TMS
$(\text{CH}_3)_3\text{SiSi}(\text{CH}_3)_3$	hexamethyldisilane	HMDS
$\overbrace{\text{CH}_2\text{SiH}(\text{CH}_3)\text{CH}_2\text{SiH}(\text{CH}_3)}$	1,3-dimethyl-1,3-disilacyclobutane	DMDSCB

## 2.1 Formation of 1,1,2,2-tetramethyldisilane (TMDS) at low filament temperatures - involvement of dimethylsilylene

As mentioned above, the gas-phase chemistry of DMS was dominated by the peak at  $m/z$  118 at a relatively low temperature and a short filament-on time. Based on the possible reaction mechanism (biradical combination reaction in Eqn. 3 and silylene insertion reaction in Eqn. 4) and its mass, this peak was assigned to 1,1,2,2-tetramethyldisilane (TMDS).



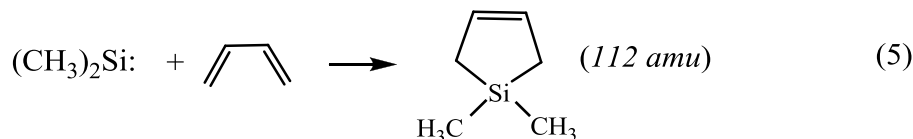
In order to confirm the nature of this peak being TMDS, the mass spectrum of 0.48 Torr of DMS at 1200 °C was compared to the room-temperature mass spectrum of an authentic TMDS sample purchased from Santa Cruz Biotechnology. This is illustrated in Figure 4. From the authentic TMDS sample, two photofragment ions, *i.e.*,  $\text{Si}(\text{CH}_3)_3^+$  ( $m/z$  73) and  $(\text{CH}_3)_2\text{SiHSiH}(\text{CH}_3)^+$  ( $m/z$

103), were observed along with the molecular ion peak at  $m/z$  118 (base peak) in the region with  $m/z > 60$ . The intensity ratios of  $I(m/z\ 73)/I(m/z\ 118)$  and  $I(m/z\ 103)/I(m/z\ 118)$  were found to be  $0.34 \pm 0.01$  and  $0.039 \pm 0.008$ , respectively. These ratios were similar in values to those obtained from the experiments using 0.12 Torr and 0.48 Torr of DMS after the filament was turned on at low filament temperatures and short time. Therefore, the identity of the peak at  $m/z$  118 is confirmed as TMDS.

Furthermore, the same experiments were performed using the deuterated isotopomer, DMS- $d_2$ . Figure 5 shows the mass spectrum of 12 Torr of 4% DMS- $d_2$ /He mixture recorded at a Ta filament temperature of 1200 °C. When DMS- $d_2$  was used, the peak at  $m/z$  118 was clearly shifted to  $m/z$  120, and the dominance of the peak at  $m/z$  120 is preserved in the spectra after turning the filament on. The corresponding photofragment ions from TMDS are now shifted to  $m/z$  73 and  $m/z$  105, as expected. This provides further support that the peak at  $m/z$  118 is indeed originated from TMDS. The formation of TMDS can proceed via two pathways, either radical recombination reaction (Eqn. 3) or silylene insertion reaction (Eqn. 4). Upon the usage of DMS- $d_2$ , both reaction mechanisms will yield the same product,  $(CH_3)_2SiDSiD(CH_3)_2$  (120 amu). This has clearly been shown in Figure 5. Although the identity of this product has been further confirmed, the exact mechanism for its formation cannot be differentiated when using the DMS- $d_2$  sample.

In order to identify the mechanism responsible for the production of TMDS, chemical trapping experiments of the active intermediates using 1,3-butadiene (BTD) were carried out. These experiments were performed using the mixture of DMS with 8-fold of BTD. Prior to each run with the mixture, a control experiment with 1% DMS and 8% BTD trapping agent, respectively, was done separately as a reference under the same experimental conditions. Figure

6 shows the TOF mass spectrum of 12 Torr of 8% BTD : 1% DMS in helium recorded at a Ta filament temperature of 1200 °C after one hour of reaction time. BTD is known as an excellent silylene trap.<sup>2,29</sup> They react to form a five-membered-ring adduct.<sup>30</sup> The reaction between dimethylsilylene and BTD, represented in Eqn. 5, leads to the formation of 1,1-dimethylsilacyclopent-3-ene with a mass of 112 amu.



The control experiment using 8% BTD performed under the same experimental conditions shows that this molecule is relatively stable at 1200 °C and does not decompose to form new species (See Figure 1 in Support Information).

As shown in Figure 2a, in the absence of BTD, the TMDS peak at  $m/z$  118 predominates the reaction products at 1200 °C. Upon the addition of this trapping agent, the peak at  $m/z$  118 was completely suppressed and a new peak representing the adduct at  $m/z$  112 appeared instead. The intensity of the peak at  $m/z$  112 increased with increasing reaction time at this temperature (Figure 6 inset), indicating that the trapping of dimethylsilylene by BTD was effective. This has led us to conclude that the product of 1,1,2,2-tetramethyldisilane is originated from the insertion reaction of dimethylsilylene into the Si-H bond in the parent DMS molecule.

Another observation is that, at the reaction time of 1 hour, the peak at  $m/z$  73 is still present. Its peak intensity distribution in the presence of BTD is also plotted in Figure 6 inset. Comparison with the same peak intensity distribution without BTD in Figure 2a shows that the intensity was suppressed, but not significantly. The decrease in its intensity with the addition of BTD is due to it being a photofragment of TMDS which is completely suppressed. Therefore,

part of the peak intensity at  $m/z$  73 should come from a new product. As will be discussed in the next section, this product is formed by a radical recombination reaction. This indicates that BTD does not react with the free radicals. An important conclusion then follows that Eqn. 3 involving free radicals does not contribute to the formation of TMDS. TMDS is formed exclusively from the silylene insertion reaction in Eqn. 4.

## 2.2 Formation of trimethylsilane (TriMS) at high filament temperatures - contribution of free radicals

After the filament was turned on when using DMS in the reactor, a distinct increase in the peak intensity at  $m/z$  73 was observed with increasing filament temperatures, as shown in Figure 3. This peak started to appear at 1200 °C. At this temperature, as discussed earlier, it has a contribution from the photofragment of the TMDS ion ( $m/z$  118). An examination of the ratio of the peak at  $m/z$  73 to the one for  $m/z$  118 showed that it varied from 0.31 to 0.98 at 1200 °C. The lower value of the ratio is comparable to one obtained from the authentic TMDS sample. The increase in the value indicates that additional factors are contributing to the intensity of this peak. At 1300 °C and beyond, the peak at  $m/z$  73 surpasses those at  $m/z$  116 and 118 at longer reaction time, and becomes the dominant peak in the mass region above 60 amu. Along with it, it is interesting to note that the  $\text{Si}(\text{CH}_3)_2^+$  peak ( $m/z$  58, the major photofragment peak of DMS) did not decrease proportionally with the DMS molecular ion ( $m/z$  60). The intensity ratio of  $I(m/z$  58)/ $I(m/z$  60) at 1200 °C was found to be higher than that at room-temperature ( $2.13 \pm 0.09$ ), and the increase is more accentuated as the filament temperature is increased (See Figure 2 in the Support Information).

From our previous study on TriMS,<sup>12</sup> it is known that its room-temperature mass spectrum is dominated by two mass peaks at  $m/z$  58 and 73 (base peak) with the intensity of the former to be 35% that of the base peak. The increase in the peak intensity at  $m/z$  58 accompanying the one at  $m/z$  73 strongly indicates that the peak at  $m/z$  73 observed in our experiment is likely originated from TriMS. Its formation involves the radical recombination reaction between methyl and dimethylsilyl radicals formed from the hot wire activation, as illustrated by Eqn. 6.



When using TriMS as the source gas in the same reactor, two major products, *i.e.*, tetramethylsilane (TMS,  $m/z$  88) and hexamethyldisilane (HMDS,  $m/z$  146), were produced.<sup>12</sup> Both of these peaks were observed in our experiments with DMS, when the peak at  $m/z$  73 increased distinctly. The detection of these two peaks presents a further confirmation on the production of TriMS in our current experiment.

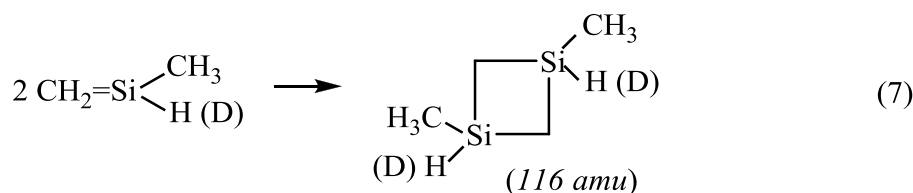
Both TriMS and its secondary reaction products (TMS and HMDS) produce a common fragment peak  $\text{Si}(\text{CH}_3)_3^+$  ( $m/z$  73) upon irradiation with the 10.5 eV VUV photons. In addition, as shown in Figure 4, TMDS also produced a significant amount of  $\text{Si}(\text{CH}_3)_3^+$  fragment (34.0% of the parent ion peak at  $m/z$  118) when subjected to the 10.5 eV photon ionization. From the room-temperature mass spectra of TMS<sup>14</sup> and HMDS<sup>23</sup>, we determined that the intensity of  $\text{Si}(\text{CH}_3)_3^+$  fragment peak is 400% and 15.3%, respectively, of the parent ion intensity of TMS ( $m/z$  88) and HMDS ( $m/z$  146). To confirm that it is TMS and HMDS that are produced with TriMS, we calculated the combined contributions to the peak intensity at  $m/z$  73 from all sources, including the photofragmentation from TriMS, TMS, HMDS, and TMDS, at different filament temperatures and filament-on time. These values were obtained by using the observed



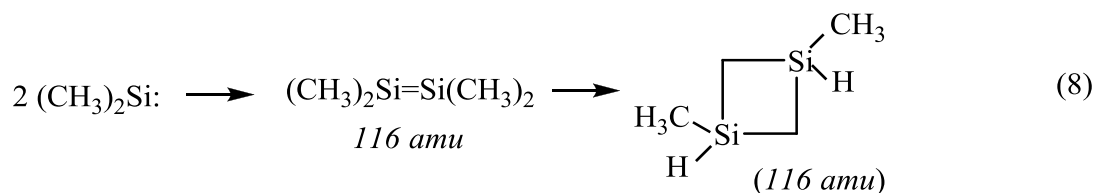
intensity of TMS, HMDS and TMDS parent ions and the peak at  $m/z$  58 from TriMS as well as the respective intensity ratios in the room-temperature mass spectra. It should be noted that, for the peak at  $m/z$  58, its net intensity was used by subtracting the contribution from the photofragments of DMS from the observed intensity. These calculated intensities are shown in Figure 7 for the temperature of 1200, 1300 and 1400 °C. The intensity profiles of the peak at  $m/z$  73 obtained from the experiments are shown in the same figure for comparison. The close agreements in the intensities computed theoretically and those obtained experimentally provide a strong support for our conclusion that trimethylsilane is produced in the reactor when using DMS as the source gas. The fact that the peak at  $m/z$  73 survives the addition of BTM, the trapping agent, indicates that its formation does not involve silylene/silene intermediates, but has the contribution from free radicals, as represented in Eqn. 6.

### **2.3 Formation of 1,3-dimethyl-1,3-disilacyclobutane (DMDSCB) at high filament temperatures**

In our experiments with DMS as the source gas, a peak at  $m/z$  116 started to appear weakly at the filament temperature of 1200 °C. This peak surpasses the one at  $m/z$  118 representing TMDS at a filament temperature of 1400 °C and higher after a reaction time of 10 - 25 min. This peak is assigned to 1,3-dimethyl-1,3-disilacyclobutane (DMDSCB). As mentioned in Section 1, H<sub>2</sub> elimination from the decomposition of DMS on the hot Ta filament produced dimethylsilylene ((CH<sub>3</sub>)<sub>2</sub>Si:) and 1-methylsilene (CH<sub>3</sub>SiH=CH<sub>2</sub>) species. 1-Methylsilene is known to be stable only under argon matrix at 10 K, and when the temperature is increased, it undergoes cyclodimerization to form DMDSCB ( $m/z$  116).<sup>31</sup> This is represented in Eqn. 7.



Conlin *et al.*<sup>32</sup> reported the evidence that dimethylsilylene can dimerize to form 1,1,2,2-tetramethyldisilene, which in turn undergoes rearrangement to produce DMDSCB, as shown in Eqn. 8.



Fortunately, the use of dideuterio-dimethylsilane (DMS-d<sub>2</sub>) would result in different mass shift in DMDSCB if it were to be formed by the two different pathways. A mass shift from 116 to 118 amu would be observed for the cyclodimerization reaction of methylsilylene, whereas the mass of DMDSCB from the dimerization reaction of dimethylsilylene would remain at 116 amu.

Figure 8 shows a comparison between the mass spectra recorded with 12 Torr of 4% DMS/He sample and 12 Torr of 4% DMS-d<sub>2</sub> sample in the reactor at a filament temperature of 1300 °C in the mass region of 110 - 126 amu. It can be noticed that the dominance of the peak at *m/z* 116 is preserved when using DMS-d<sub>2</sub>, but shifted by 2 amu to a peak at *m/z* 118. To better illustrate this preservation of dominance, the intensity distribution of peaks at *m/z* 116, 118 and 120 originated from DMS-d<sub>2</sub> is plotted and compared to the one for the peaks at *m/z* 116 and 118 obtained from DMS. They are shown in Figure 9. The intensity of the peak at *m/z* 116 is higher than the one for the peak at *m/z* 118 when using DMS. The same trend is observed when the isotopomer was used where the peak at *m/z* 118 is dominating over the one at *m/z* 120. This clearly suggests that the dimerization of 1-methylsilylene (Eqn. 7) is responsible for forming

DMSDSCB ( $m/z$  116). However, it should be noted that the peak at  $m/z$  116 did not disappear when DMS- $d_2$  was used, indicating the occurrence of dimethylsilylene dimerization (Eqn. 8). The intensity ratio of  $I(m/z$  116)/ $I(m/z$  118) with the DMS- $d_2$  sample ranges from 0.24 to 0.62. Therefore, it can be concluded that both silene dimerization and silylene dimerization contribute to the formation of DMDCSB. Since the intensity ratio of  $I(m/z$  116)/ $I(m/z$  118) is less than 1, cycloaddition of 1-methylsilene is the dominate mechanism.

To confirm the mechanism accountable for the formation of DMDCSB, trapping experiments with BTD were carried out at a filament temperature of 1400 °C, since the peak at  $m/z$  116 was dominating over the one at  $m/z$  73 at this temperature. In addition to the reaction with a silylene species as shown in Eqn. 5, BTD is also known to react with silene to form a six-membered-ring compound.<sup>29,3</sup> Eqn. 9 shows such a reaction between BTD and 1-methylsilene, forming 1-methylsilacyclohex-3-ene with a mass of 112 amu.

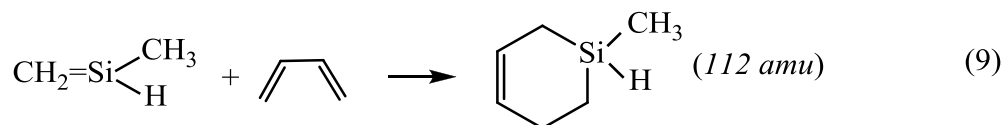


Figure 10 illustrates the mass spectrum recorded at a filament temperature of 1400 °C using the mixture of 8% BTD and 1% DMS in He. Both peaks at  $m/z$  118 and 116 that were present in the absence of BTD disappeared upon the addition of BTD. Along with it, the peak at  $m/z$  112 representing the trapping adduct was observed. The reactions between the trapping agent BTD and methylsilene/dimethylsilylene intermediates result in the formation of two different adducts with the same mass, as represented by Eqns. 5 and 9. Therefore, the usage of BTD did not help in differentiating between the two routes responsible for the formation of DMDCSB. However, the appearance of the adduct peak confirms that DMDCSB is originating from silene/silylene chemistry, not from reactions involving free radicals. The new peak at  $m/z$  112

increases with increasing reaction time as shown in the inset of Figure 10. The peak at  $m/z$  73 representing TriMS produced from the radical recombination reaction (Eqn. 6) survived the addition of BTB. Its intensity distribution at 1400 °C, also shown in Figure 10 inset, indicates an increase with time. This agrees well with the trend observed in the absence of BTB at the same temperature (Figure 3 b). It is worth mentioning that at this high temperature, the control experiment with 8% BTB showed the appearance of new peaks at  $m/z$  66, 68, 70, 78, 80, 81, 82, 84, 95 and 110 resulting from the decomposition of BTB at 1400 °C (See Figure 3 in Support Information). These peaks did not overlap with any of the peaks related to DMS chemistry.

In summary, the involvement of free radicals and silene/silylene intermediates in the gas-phase chemistry of DMS is portrayed by the presence of the peaks at  $m/z$  73, 118 and 116. As it has been demonstrated, the gas-phase chemistry of DMS is dominated by the formation of 1,1,2,2-tetramethyldisilane (TMDS) at low filament temperatures and short reaction time. With the help of trapping experiments with 1,3-butadiene, it was confirmed that the formation of this molecule involves the insertion reaction of dimethylsilylene into Si-H bond of the parent DMS molecule. As the temperature is increased to 1300 and 1400 °C and at long reaction time, the peaks at  $m/z$  73 and 116 predominate. The peak at  $m/z$  73 was assigned to trimethylsilane (TriMS), a product from radical recombination reaction between methyl and dimethylsilyl radicals. The detection of the peak at  $m/z$  116 indicate the formation of 1,3-dimethyl-1,3-disilacyclobutane (DMDSCB). From the isotope labeling experiment as well as the trapping experiment with 1,3-butadiene, it was concluded that the formation of this peak proceeds via methylsilylene cyclodimerization reaction and dimethylsilylene dimerization reaction, with the former being more important. At even higher temperatures of 1500 and 1600 °C, TriMS becomes the dominant product at all time. Therefore, unlike TriMS<sup>12</sup> and TMS<sup>14</sup> where free-radical

reactions predominate the secondary gas-phase reactions, with increasing number of Si-H bonds in DMS, there is a competition between reactions involving silylene and free radical intermediates when DMS is used as a precursor gas in a hot-wire CVD reactor. Specifically, silylene insertion reaction dominates at low filament temperatures, whereas free radical reactions become important only at high temperatures.

### 3. Effect of filament material on DMS gas-phase chemistry

The nature of the filament material is believed to play a role in the decomposition of the gas precursors in the HWCVD system. In the study of the influence of filament material on the deposition of polycrystalline Si thin films using  $\text{SiH}_4/\text{H}_2$  mixture,<sup>33</sup> it was found that thin films grown by hot-wire CVD using W and Ta as filament materials show different material properties, and this difference is caused by the different surface reaction and catalytic properties of the filament material. Duan *et al.*<sup>34</sup> has studied the effect of filament material on the decomposition of  $\text{SiH}_4$  by monitoring the production of Si radical from W, Re, Mo and Ta filaments. Their results showed that the different material provided different apparent activation energy values for Si formation, suggesting that different mechanisms may be active. For the influence of filament material on the deposition of  $\text{Si}_{1-x}\text{C}_x$  thin films using DMS, as mentioned in the introduction, Nakayama *et al.*<sup>9</sup> found that Mo and Pt produced large precursors leading to high carbon content in the film, while W and Ta decomposed DMS to form small precursors, reducing the carbon composition in the film. Hence, as the key component in hot-wire CVD is the filament at which the catalytic decomposition of the source gas occurs, the possible use of different materials, including W and Ta, and their influence on the gas-phase reaction chemistry are investigated.

From the previous discussions, it was concluded that the secondary gas-phase reactions of DMS on a Ta filament are dominated by the formation of three major products, *i.e.*, trimethylsilane (TriMS) at  $m/z$  73, 1,1,2,2-tetramethyldisilane (TMDS) at  $m/z$  118, and 1,3-dimethyl-1,3-disilacyclobutane (DMDS) at  $m/z$  116. When replacing the Ta with a W filament and performing the same experiments, the same three products have been detected. A slight difference in the temperature at which the gas-phase chemistry becomes active was observed for the two filaments. This is shown in Table 2. However, at higher temperatures, the intensity distributions for the three product peaks at  $m/z$  73, 116, and 118 are very similar. An example is shown for a filament temperature of 1500 °C in Figure 11 when using 0.12 Torr of DMS sample on the two filaments.

Table 2. The filament temperature at which the gas-phase reaction chemistry becomes active for Ta and W filaments

Sample	Filament Material	Starting temperature (°C )
0.12 Torr DMS	Ta	1100
0.12 Torr DMS	W	1200
0.48 Torr DMS	Ta	1000
0.48 Torr DMS	W	1100

The similarity in the gas-phase chemistry when using DMS on the two filaments (Ta and W) is quite different from the observed difference in the Si radical formation<sup>34</sup> and deposited Si film properties<sup>33</sup> when using SiH<sub>4</sub>. Our previous study on the decomposition of methyl-substituted silanes, including DMS, on a metal surface<sup>26</sup> has shown that it is initiated by the same rate-limiting step, *i.e.*, the cleavage of the Si-H bond, on both Ta and W filaments. The formation

of H<sub>2</sub> occurs by the recombination reaction between two H adsorbates, following Langmuir-Hinshelwood mechanism. The rupture of the Si-CH<sub>3</sub> bond results in the release of the methyl radical into the gas phase. The activation energy for the formation of H<sub>2</sub> (or ·CH<sub>3</sub>) from DMS is comparable on both filaments. This agrees well with the observed similarity with Ta and W in the DMS reaction chemistry in a hot-wire CVD reactor. Therefore, it can be concluded that the decomposition chemistry of source gas molecules on the metal filament surfaces plays a key role in determining the subsequent secondary gas-phase reactions in the reactor that produce the actual film growth precursors, and consequently the deposited thin film properties.

For a rational optimization of the HWCVD process for high-quality thin films for industrial applications, it is important to establish a comprehensive deposition model that incorporates the gas-phase reaction chemistry, the film growth chemistry, the reactor geometry, and process parameters. A lot of work has been performed on modeling and simulation of the formation of various materials such as carbon/carbon composites,<sup>35</sup> diamond,<sup>36</sup> and CdTe<sup>37</sup> using CVD methods. Most of the work on simulation of HWCVD of Si-containing thin films focuses on the deposition of silicon from SiH<sub>4</sub><sup>38,39</sup> and on silicon carbide from SiH<sub>4</sub> and C<sub>3</sub>H<sub>8</sub> mixtures.<sup>40,41</sup> All emphasize the importance and need to include accurate and complete reaction mechanisms for the decomposition of source gases on the hot wire, the gas-phase reactions, and the film-growth reactions on the substrate surfaces. There is, in general, a lack of study on the modeling of single-source precursors for the deposition of silicon carbide. In their work on the modeling of silicon carbide deposition in a low-pressure CVD (LPCVD) reactor using the single-source precursor of 1,3-disilabutane (CH<sub>3</sub>SiH<sub>2</sub>CH<sub>2</sub>SiH<sub>3</sub>), Valente *et al.*<sup>42</sup> investigated the reaction pathways both in the gas phase and on the substrate surface in order to explain the profiles of growth rate under different process conditions. They showed that the most important

reaction in the gas phase in the decomposition of 1,3-disilabutane to produce a diradical silylene species,  $\text{CH}_3\text{SiH}_2\text{CH}_2(\text{H})\text{Si}\cdot$ . The presence of this growth precursor in addition to 1,3-disilabutane explains the growth rate profiles observed experimentally. Our current work on the decomposition of DMS in a HWCVD reactor also showed the dominance of silylene chemistry at filament temperatures of 1100-1200 °C, in agreement with the study on 1,3-disilabutane. It is hoped that our study reported here on the gas-phase reaction chemistry with DMS will provide the detailed reaction mechanisms on which a theoretical model can be based - the first step toward the effort of establishing a comprehensive model using this single-source gas.

## Conclusions

In this work, the primary decomposition of dimethylsilane (DMS) on a hot W or Ta filament and secondary gas-phase reactions in a hot-wire CVD reactor was explored using laser ionization mass spectrometry. Under the collision-free conditions, DMS decomposes on a metal filament (W or Ta) to form  $\text{H}_2$  molecule and two radicals ( $\cdot\text{CH}_3$  and  $\cdot\text{H}$ ) along with the co-products, dimethylsilyl radical ( $\cdot\text{SiH}(\text{CH}_3)_2$ ), dimethylsilylene ( $(\text{CH}_3)_2\text{Si}\cdot$ ), and 1-methylsilylene ( $(\text{CH}_3)\text{HSi}=\text{CH}_2$ ). Our study of the gas-phase reaction chemistry of DMS in a hot-wire CVD reactor has demonstrated that both free radical and silylene/silene intermediates play important roles. The competition between the free-radical reactions and those involving silylene/silene species depends on the filament temperature and reaction time. At low filament temperatures of 1100-1200 °C, the secondary gas-phase reactions are dominated by the insertion of dimethylsilylene into the Si-H bond of the parent DMS molecule, forming 1,1,2,2-tetramethyl-disilane (TMDS,  $m/z$  118). As the filament temperature and reaction time is increased, free radical recombination reactions become more important. This leads to the predominance of the



formation of trimethylsilane (TriMS,  $m/z$  73) at 1500 - 1600 °C. It has also been demonstrated that 1,1-dimethyl-1,3-disilacyclobutane (DMDSCB,  $m/z$  116) is produced in the reactor when using DMS as a source gas. This species is believed to be formed from the cyclodimerization reactions of 1-methylsilene and also from dimethylsilylene dimerization. The formation mechanism of the three major products were confirmed by using the deuterated isotopomer, DMS- $d_2$ , as well as chemical trapping with 1,3-butadiene.

With an increase number of Si-H bond in DMS as compared to TriMS and TMS, significant difference has been observed in the reaction chemistry in the environment of a hot-wire CVD reactor. The temperature at which the reactions become active in the reactor is lowered when using DMS. Furthermore, reactions involving silylene/silene intermediates are the dominant mechanism operating at low filament temperatures and short reaction time. This is quite different from the observations with TriMS and TMS where the involvement of silene intermediates is important only at high temperatures ( $T \geq 1600$  °C) with a minor contribution. The free-radical reaction, which dominates the reaction chemistry with TriMS and TMS, also occur when DMS is used. However, it only become dominant when the filament temperature is increased to 1500 - 1600 °C. Based on these results, it is expected that the silicon carbide films deposited using DMS and TMS (or TriMS) would show different properties since the actual film growth precursors formed in the gas phase are different. Filament temperature is a key parameter to show the difference. Our current work on the effect of filament material, W vs. Ta, has shown that the same reaction chemistry is observed on the two filaments. Therefore, although we predict that the structure of the source gas used would affect the film properties, the use of different filament material of W and Ta should not change much the deposited silicon carbon thin film property when using DMS as the source gas.

### **Acknowledgements**

The financial support for this work by Natural Sciences and Engineering Research Council of Canada (NSERC) is gratefully acknowledged.

## References

1. P. S. Neudorfl and O. P. Strausz, *J. Phys. Chem.*, 1978, **82**, 241-242.
2. M. A. Ring, H. E. Oneal, S. F. Rickborn and B. A. Sawrey, *Organometal.*, 1983, **2**, 1891-1894.
3. S. F. Rickborn, D. S. Rogers, M. A. Ring, and H. E. Oneal, *J. Phys. Chem.*, 1986, **90**, 408-414.
4. H. E. Oneal and M. A. Ring, *Organometal.*, 1988, **7**, 1017-1025.
5. A. G. Alexander and O. P. Strausz, *J. Phys. Chem.*, 1976, **80**, 2531-2538.
6. K. Yasui, K. Asada and T. Akahane, *Appl. Surf. Sci.*, 2000, **159**, 556-560.
7. Y. Narita, T. Inubushi, K. Yasui and T. Akahane, *Appl. Surf. Sci.*, 2003, **212**, 730-734.
8. Y. Narita, M. Harashima, K. Yasui, T. Akahane and M. Takata, *Appl. Surf. Sci.*, 2006, **252**, 3460-3465.
9. H. Nakayama, K. Takatsuji, K. Murakami, Y. Miura, N. Shimoyama and H. Machida, *Thin Solid Films*, 2003, **430**, 87-90.
10. G. A. Zaharias, H. L. Duan and S. F. Bent, *J. Vac. Sci. Technol. A*, 2006, **24**, 542-549.
11. Lee, M. S.; Bent, S. F., *J. Vac. Sci. Technol. A*, 1998, **16**, 1658-1663.
12. Shi, Y. J.; Li, X. M.; Toukabri, R.; Tong, L., *J. Phys. Chem. A*, 2011, **115**, 10290-10298.
13. R. Toukabri and Y. J. Shi, *J. Vac. Sci. Technol. A*, 2013, **31**, 061606-1 - 6.
14. X. M. Li, B. D. Eustergerling and Y. J. Shi, *Int. J. Mass Spectrom.*, 2007, **263**, 233-242.
15. J. K. Holt, M. Swiatek, D. G. Goodwin and H. A. Atwater, *J. Appl. Phys.*, 2002, **92**, 4803-4808.
16. A. H. Mahan, *Sol. Energ. Mat. Sol. Cell*, 2003, **78**, 299-327.
17. L. Tong, C. E. Sveen and Y. J. Shi, *J. Appl. Phys.*, 2008, **103**, 123534-1 - 6.
18. C. E. Sveen and Y. J. Shi, *Thin Solid Films*, 2011, **519**, 4447-4450.

19. Y. Q. Xu, A. H. Mahan, L. M. Gedvilas, R. C. Reedy and H. M. Branz, *Thin Solid Films*, 2006, **501**, 198-201.
20. N. Kniffler, A. Pflueger, D. Scheller and B. Schroeder, *Thin Solid Films*. 2009, **517**, 3424-3426.
21. Y. J. Shi, S. Consta, A. K. Das, B. Mallik, D. Lacey and R. H. Lipson, *J. Chem. Phys.*, 2002, **116**, 6990-6999.
22. S. D. Chambreau and J. S. Zhang, *Chem. Phys. Lett.*, 2001, **343**, 482-488.
23. Y. J. Shi, X. M. Li, L. Tong, R. Toukabri and B. Eustergerling, *Phys. Chem. Chem. Phys.*, 2008, **10**, 2543-2551.
24. I. Badran, T. D. Forster, R. Roesler and Y. J. Shi, *J. Phys. Chem. A* 2012, **116**, 10054-10062.
25. S. Tannenbaum, S. Kaye and G. F. Lewenz, *J. Am. Chem. Soc.*, 1953, **75**, 3753-3757.
26. R. Toukabri, N. Alkadhi and Y. J. Shi, *J. Phys. Chem. A*, 2013, **117**, 7697-7704.
27. Y. J. Shi, B. Lo, L. Tong, X. Li, B. D. Eustergerling and T. S. Sorensen, *J. Mass Spectrom.*, 2007, **42**, 575-583.
28. L. Tong and Y. J. Shi, *J. Mass Spectrom.*, 2010, **45**, 215-222.
29. R. T. Conlin and R. S. Gill, *J. Am. Chem. Soc.*, 1983, **105**, 618-619.
30. M. P. Clarke and I. M. T. Davidson, *J. Chem. Soc. Chem. Comm.*, 1988, 241-243.
31. L. E. Gusel'nikov, *Coordin. Chem. Rev.*, 2003, **244**, 149-240.
32. R. T. Conlin and P. P. Gaspar, *J. Am. Chem. Soc.*, 1976, **98**, 868-870.
33. P. A. T. T. van Veenendaal, O. L. J. Gijzeman, J. K. Rath and R. E. I. Schropp, *Thin Solid Films*, 2001, **395**, 194-197.
34. H. L. Duan and S. F. Bent, *Thin Solid Films*, 2005, **485**, 126-134.

35. A. Li, K. Norinaga, W. Zhang and O. Deutschmann, *Composites Sci. Technol.* 2008, **68**, 1097-1104.
36. J. E. Butler, Y. A. Mankelevich, A. Cheesman, J. Ma and M. N. R. Ashfold, *J. Phys. Cond. Matter*, 2009, **21**, 364201-1 - 364201-20.
37. X. W. Zhou, D. K. Ward, B. M. Wong, F. P. Doty, J. A. Zimmerman, G. N. Nielson, J. L. Cruz-Campa, V. P. Gupta, J. E. Granata, J. J. Chavez and D. Zubia, *Phys. Rev. A* 2012, **85**, 245302-1- 245302-15.
38. A. Pant, M. C. Huff and T. W. F. Russell, *Ind. Eng. Chem. Res.* 2001, **40**, 1386-1396.
39. A. Pflüger, B. Schröder and H. J. Bart, *Thin Solid Films*, 2003, **430**, 73-77.
40. C. D. Stinespring and J. C. Wormhoudt, *J. Cryst. Growth*, 1988, **87**, 481-493.
41. M. D. Allendorf and R. J. Kee, *J. Electrochem. Soc.* 1991, **138**, 841-852.
42. G. Valente, M. B. J. Wijesundara, R. Maboudian and C. Carraro, *J. Electrochem. Soc.* 2004, **151**, C215-C219.

### Figure Captions

Figure 1. The Intensity ratio of a)  $(\text{CH}_3)_2\text{SiH}^+$  ( $m/z$  59) to that of the parent of  $(\text{CH}_3)_2\text{SiH}_2^+$  ( $m/z$  60), and b)  $\text{C}_2\text{H}_6\text{Si}^+$  ( $m/z$  58) to that of the parent of  $(\text{CH}_3)_2\text{SiH}_2^+$  ( $m/z$  60) for pure DMS versus the W filament temperature at a chamber pressure of  $1 \times 10^{-5}$  Torr.

Figure 2. 10.5 eV SPI TOF mass spectra of 0.12 Torr of DMS in the reactor at Ta filament temperatures between 1200 and 1600 °C. The spectrum at 25 °C is recorded when the filament is off.

Figure 3. Intensity distributions of the peaks at  $m/z$  73, 118 and 116 as a function of reaction time when using 0.12 Torr of DMS and at a Ta filament temperature of a) 1200 °C, b) 1400 °C, and c) 1600 °C.

Figure 4. 10.5 eV SPI TOF mass spectrum of 0.48 Torr of DMS sample in the reactor at a Ta filament temperature of 1100 °C in the mass region of 50 - 130 amu. The inset is a mass spectrum of an authentic TMDS sample recorded at room temperature.

Figure 5. 10.5 eV SPI TOF mass spectrum of 0.48 Torr of DMS- $d_2$  recorded 10 minutes after the Ta filament was turned on at 1200 °C.

Figure 6. 10.5 eV SPI TOF mass spectra of 12 Torr 1% DMS + 8% BTM in He in the reactor at a Ta filament temperature 1200 °C after one hour of turning the filament on (Note: the peak at  $m/z$

54 is overloaded). Inset: The intensity of peak at  $m/z$  112 and 73 from 12 Torr 8% BTD + 1% DMS/He versus filament-on time at a filament temperature of 1200 °C.

Figure 7. The intensity of the peak at  $m/z$  73 observed with 0.12 Torr DMS at 1200 °C (■), 1300 °C (●), and 1400 °C (▲). The contribution to the peak intensity from the photofragmentation of TriMS, TMS, HMDS, and TMDS combined at 1200 (□), 1300 (○) and 1400 °C (Δ) is shown for comparison.

Figure 8. 10.5 eV SPI TOF mass spectra of a) 0.48 Torr of DMS, and b) 0.48 Torr of DMS-d<sub>2</sub> in the reactor at a Ta filament temperature of 1300 °C.

Figure 9. The intensity distribution of the peaks at a)  $m/z$  116 and 118 originated from 0.48 Torr of DMS, and b)  $m/z$  116, 118 and 120 produced from 0.48 Torr of DMS-d<sub>2</sub> at a Ta filament temperature of 1300 °C.

Figure 10. 10.5 eV SPI TOF mass spectra of 12 Torr 1% DMS + 8% BTD in He in the reactor at a Ta filament temperature 1400 °C after 10 min of turning the filament on (Note the peak at  $m/z$  54 is overloaded). Inset: Intensity of peak at  $m/z$  112 and 73 from 12 Torr 8% BTD + 1% DMS/He versus filament-on time at a filament temperature of 1400 °C.

Figure 11. Intensity distributions of the peaks at  $m/z$  73, 118 and 116 when using 0.12 Torr of DMS at a filament temperature of 1500 °C on the filament of a) Ta, and b) W.

Figure 1

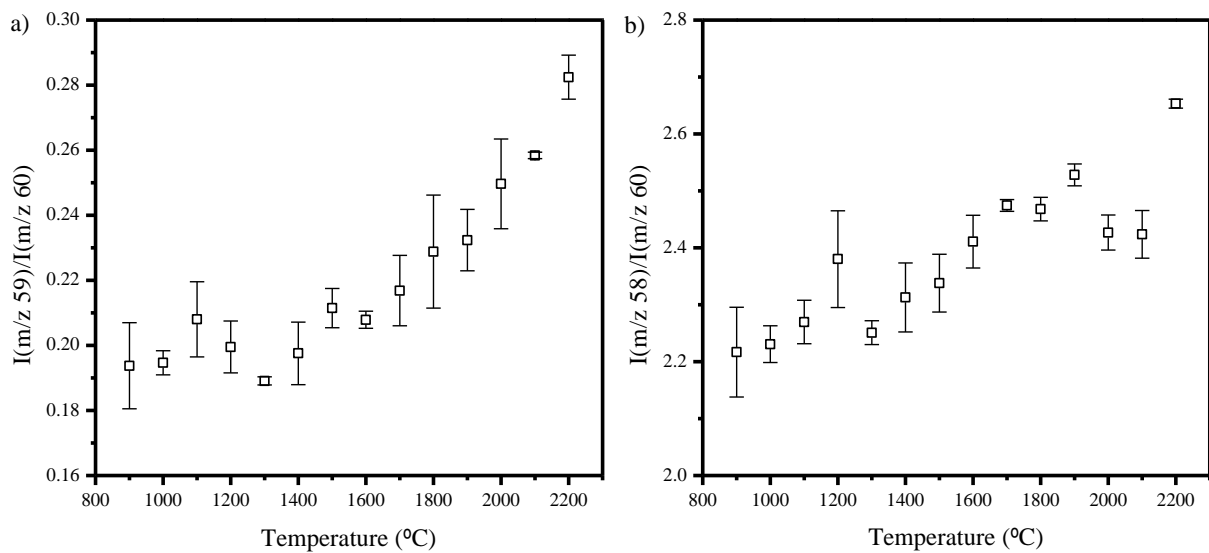




Figure 2

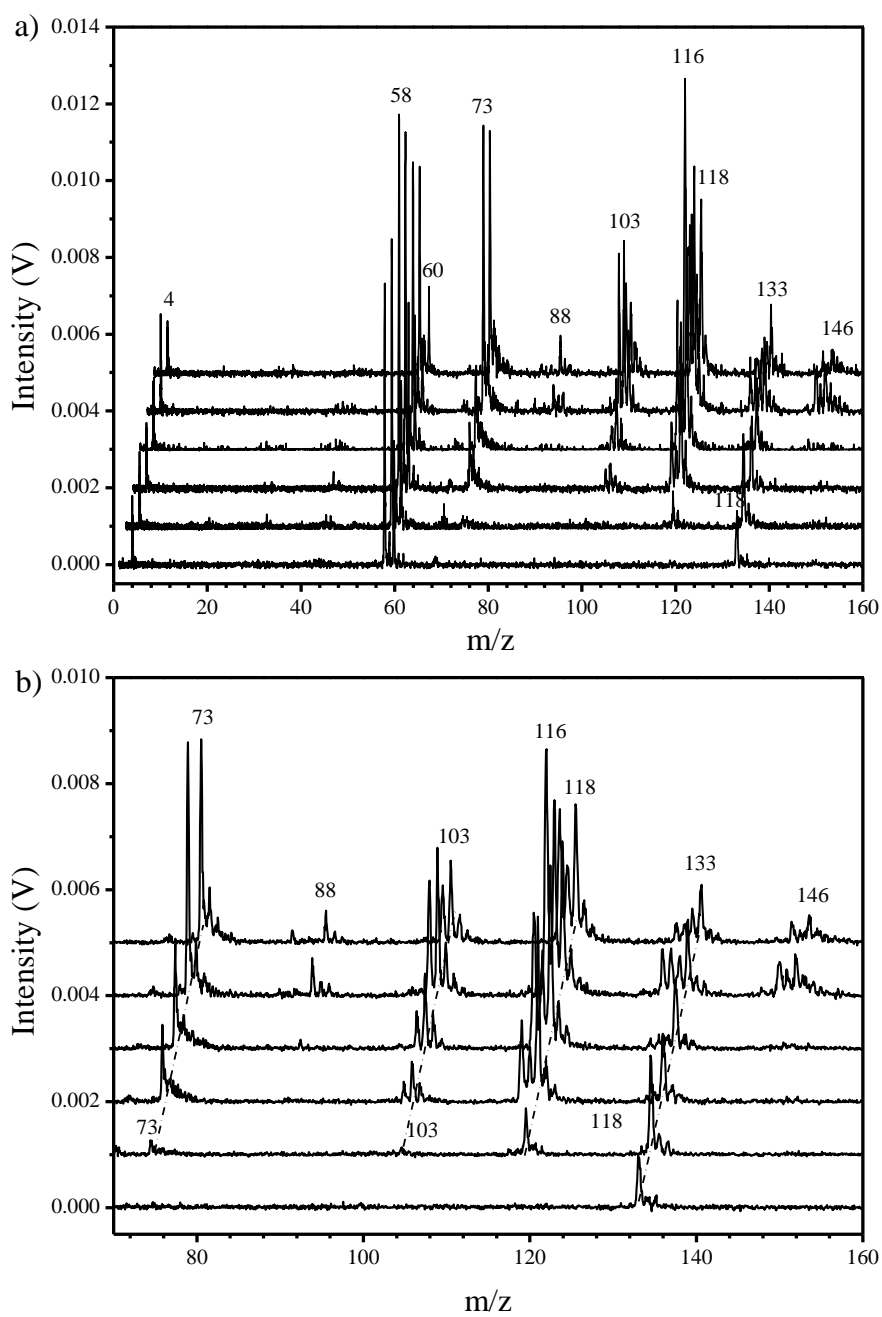


Figure 3

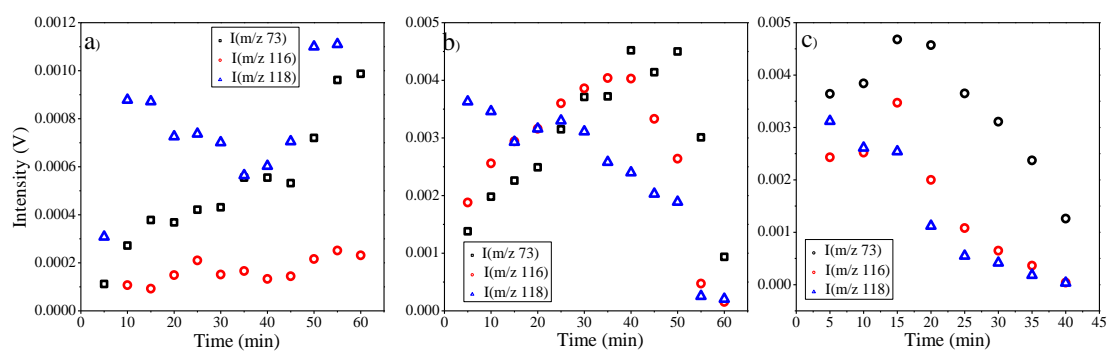


Figure 4

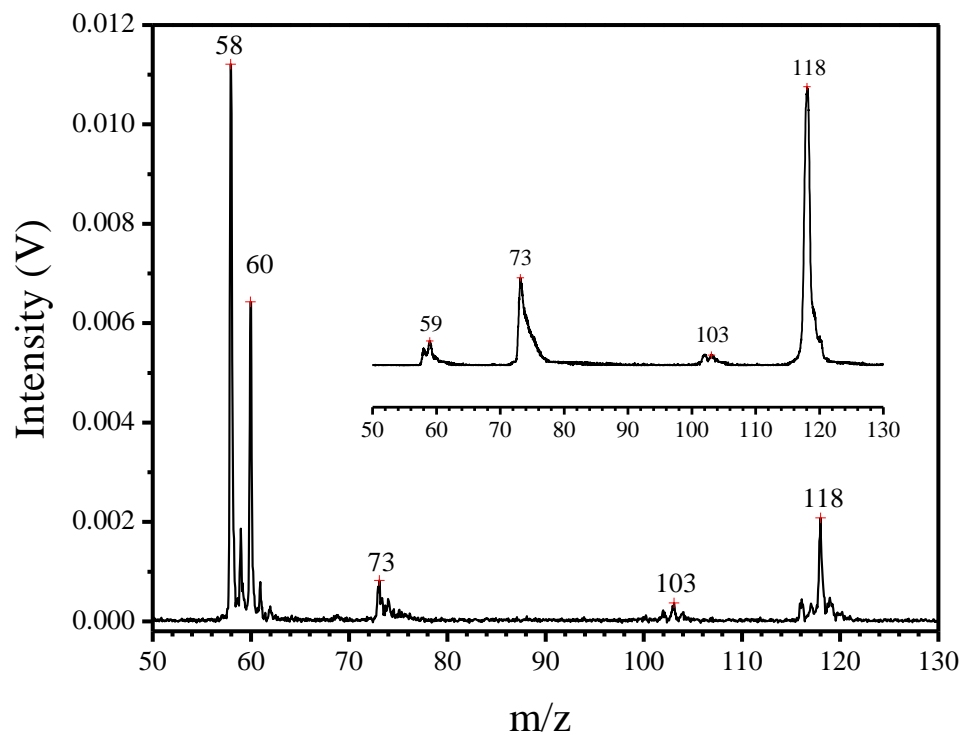


Figure 5

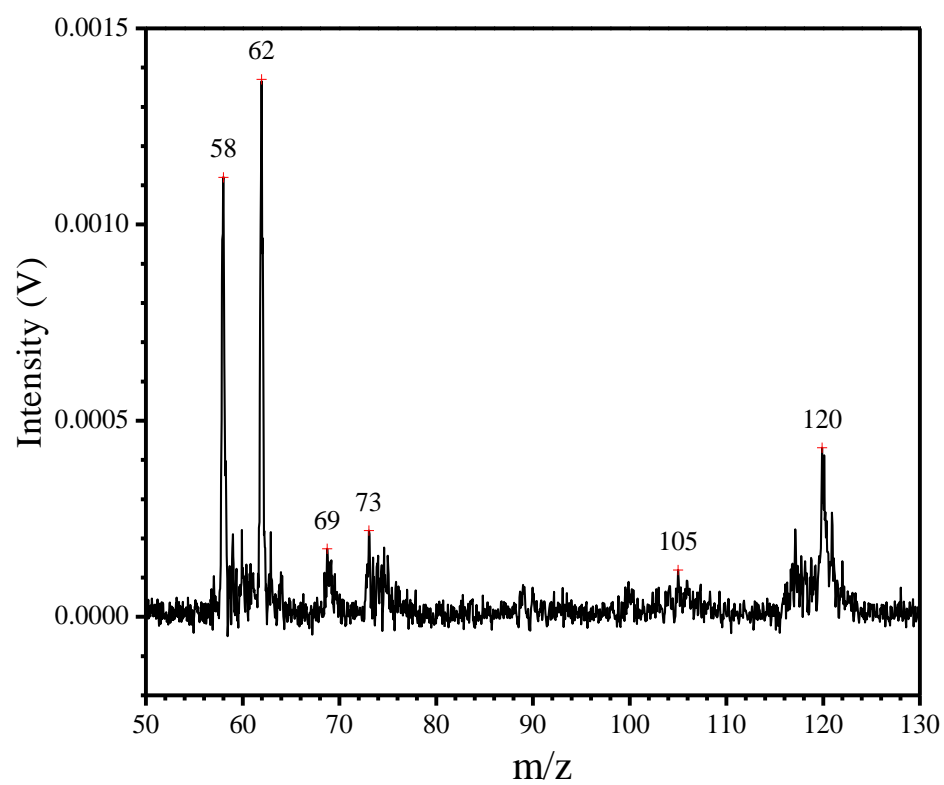


Figure 6

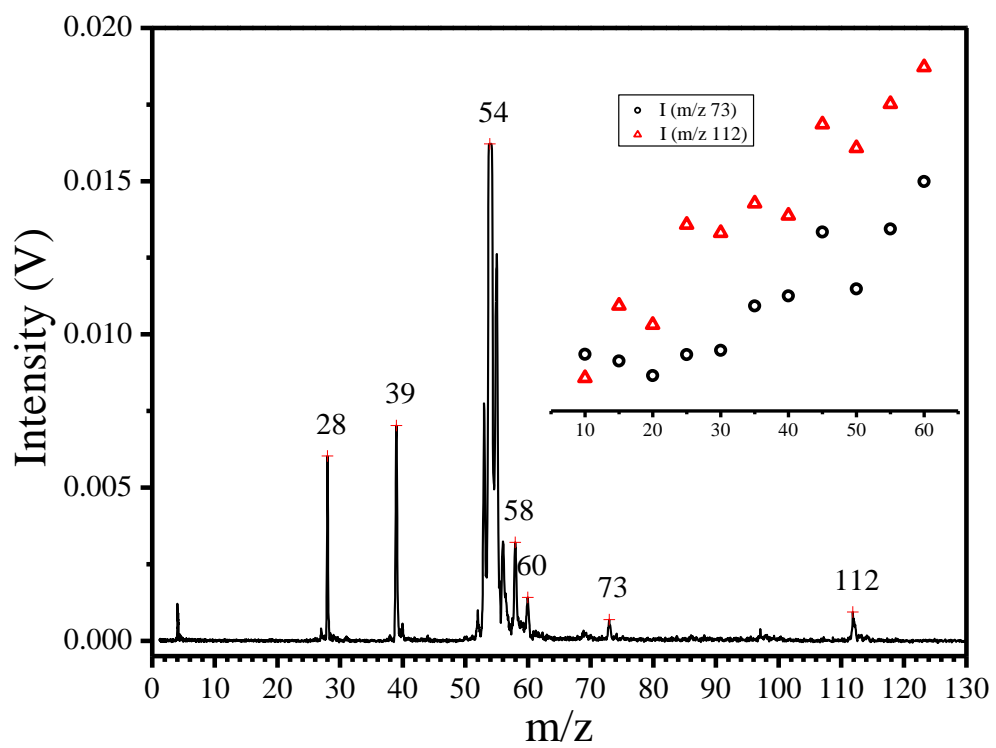


Figure 7

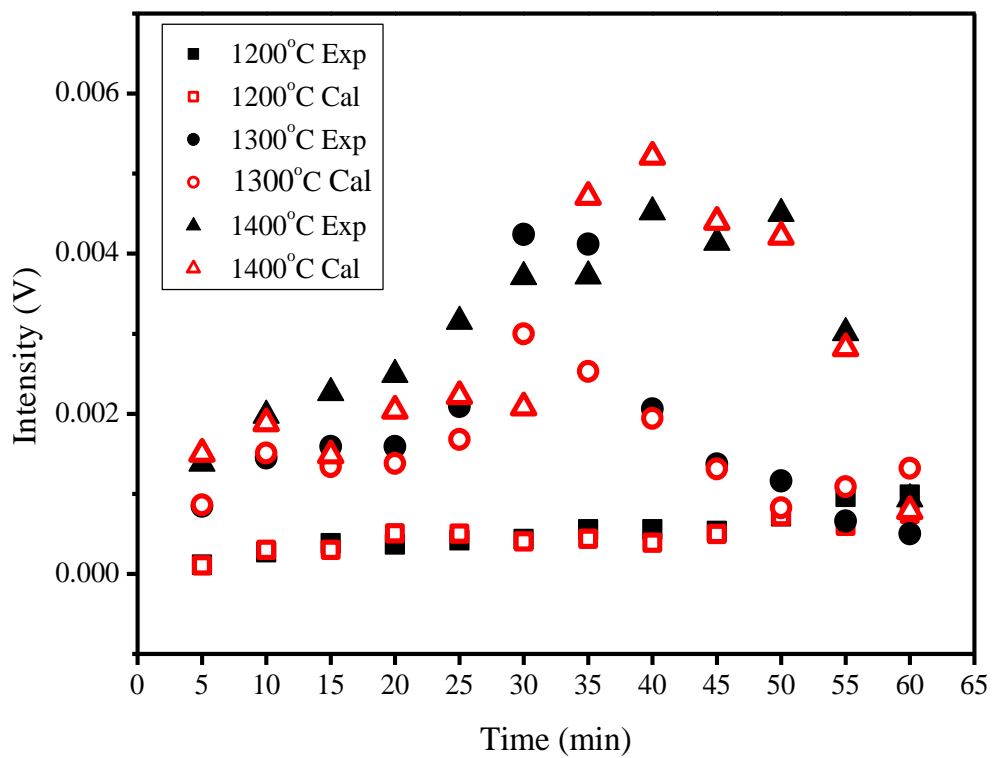


Figure 8

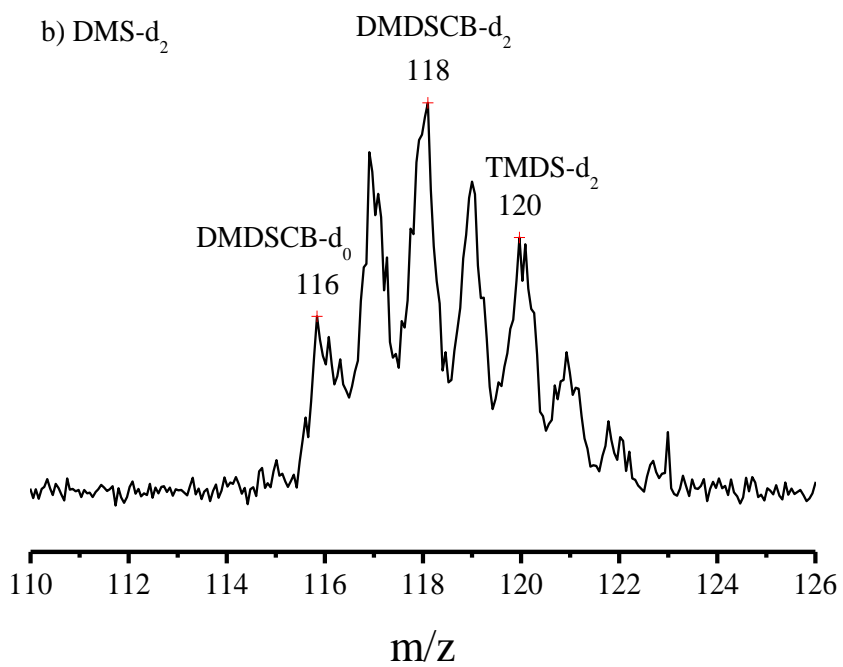
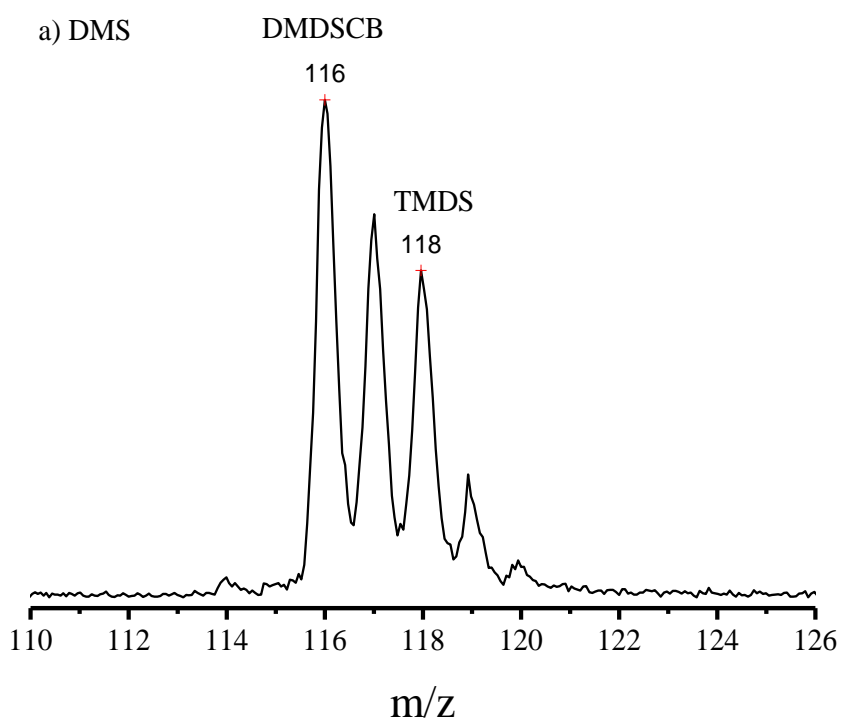


Figure 9

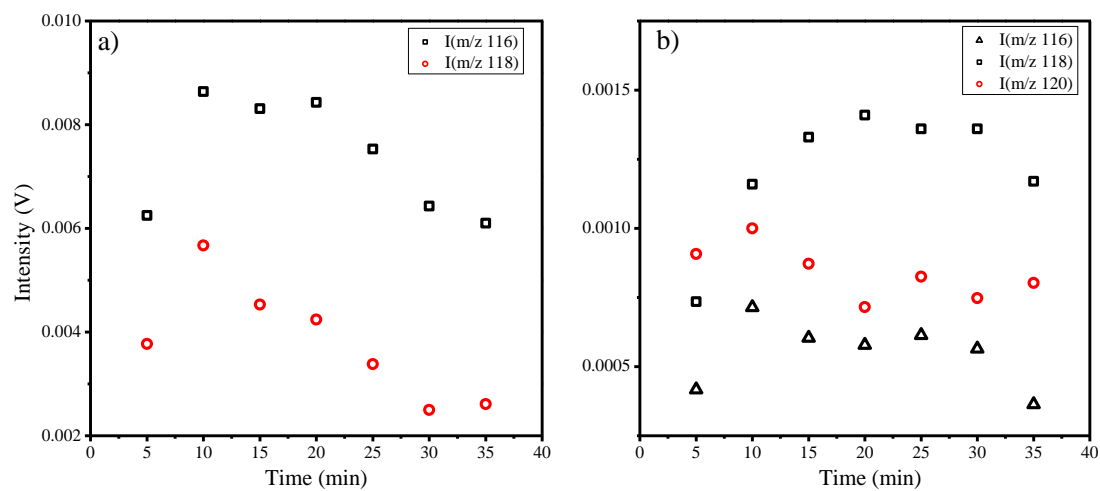




Figure 10

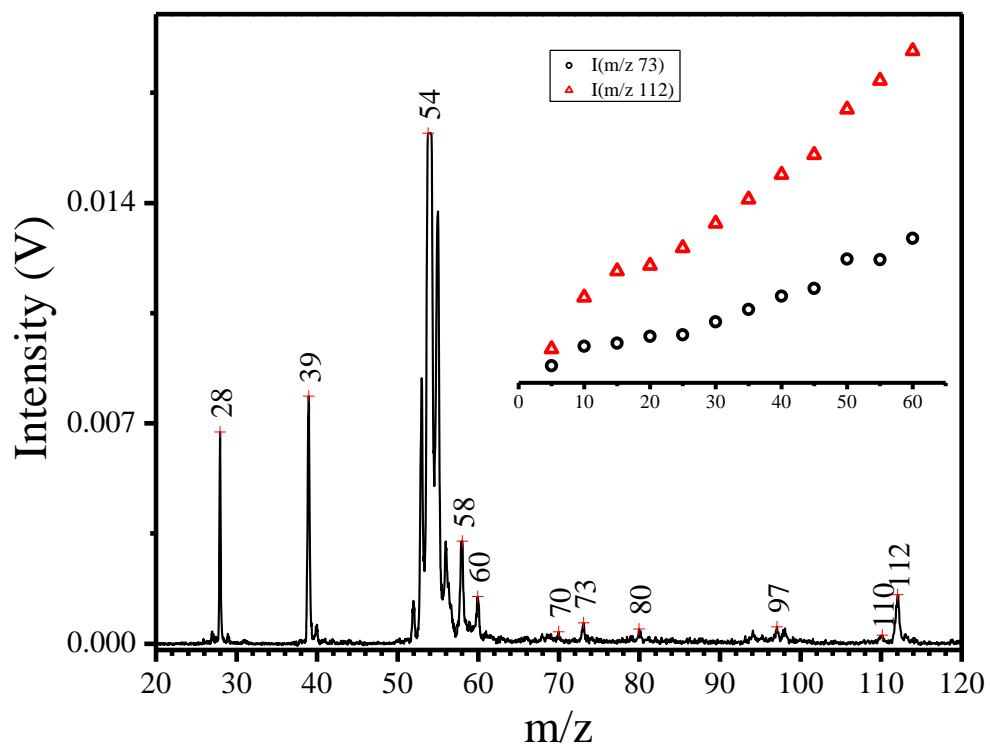


Figure 11

